In vitro behavior of HVOF sprayed calcium phosphate splats and coatings

K.A. Khor[a],*, H. Li[a], P. Cheang[b], S.Y. Boey[c]

[a] School of Mechanical & Production Engineering, Nanyang Technological University, 50, Nanyang Avenue, Singapore 639798, Singapore
[b] School of Materials Engineering, Nanyang Technological University, 50, Nanyang Avenue, Singapore 639798, Singapore
[c] Singapore Polytechnic, Dover Road, Singapore

Abstract

Hydroxyapatite (HA) coatings and splats deposited by high velocity oxy-fuel (HVOF) spray technique was investigated in vitro. HA coatings prepared from two different HA powder size range (30 ± 5 and 50 ± 5 μm) were immersed in a simulated body fluid with various incubation periods of maximum 6 weeks. The dissolution/precipitation behavior was studied and the degradation of HA coatings caused by in vitro ageing was demonstrated by measuring the changes in flexural modulus through a 3-point bend test. It was found that the dissolution and precipitation behavior of the coatings was significantly dependent upon the incipient coating phase composition and the precipitation of bone-like hydroxyapatite on the coating's surface was found to be directly related to the dissolution process. Higher dissolution rates of tricalcium phosphate, tetracalcium phosphate and amorphous calcium phosphate relative to HA, resulted in accelerated precipitation. Furthermore, analysis of coatings' surface morphology demonstrated that advanced precipitation invariably occurred at regions where dissolution took place. Results showed that the changes in flexural modulus of investigated HA coatings accompanying different incubation duration was not systematic but was found to be dependent upon changes of coating structure and other factors brought about by in vitro ageing. In vitro investigation of individual HA splats collected from different HA particle sizes revealed, after 3 days ageing, that the rate ratio of precipitation to dissolution was directly determined by the local phase composition, and this phenomenon could be effectively used to explain the behavior of thermally sprayed HA coatings in vitro. It implied that the precipitation was strongly dependent on the first molecule attachment. To achieve rapid precipitation in vitro, partial molten state of HA particles during HVOF coating deposition was recommended.
© 2002 Elsevier Science Ltd. All rights reserved.

Keywords: Hydroxyapatite; Thermal spray; Splats; In vitro; Precipitation; Dissolution

1. Introduction

Hydroxyapatite (HA) coatings deposited by thermal spray techniques onto titanium alloy substrates have been extensively investigated as implants in clinical applications. Among the coating properties relating to extensive duration and functional performance in service, the bioactivity of as sprayed HA coating, especially that demonstrated by the coating surface, and mechanical properties conduct an important role. Available studies showed that the bonding mechanism of bone with HA seemed to involve dissolution/reprecipitation phenomena [1]. And the remodeling process is fundamental for successful implant fixation

and stability in the long term [2]. It has been claimed that the behavior of the HA family upon immersion in a simulated body fluid (SBF) was structure- and composition-dependent [3]. And the coating's dissolution rate is dependent largely on the crystallinity level [4,5], phase composition, microstructure, and surface area and density [6]. Munting [7] showed that implant fixation must depend on a mechanical interlock with bone and was not related to the duration of implantation. Therefore, early dissolution/precipitation of HA coating is severely critical and the changes of mechanical properties of the HA coating need to be considered.

High velocity oxy-fuel (HVOF) spray technique has showed its capability in producing HA coatings with promising mechanical properties [8,9]. In a previous report [8], it was pointed out that the starting HA powder size played an important role in determining

*Corresponding author. Tel.: +65-7905526; fax: +65-7911859.
E-mail address: mkakhor@ntu.edu.sg (K.A. Khor).

coating properties including adhesive strength and phase composition. Partially melted HA powder could result in an almost fully crystallized structure. It was generally believed that the existence of an amorphous phase had a beneficial effect in accelerating dissolution and hence, improved bone apposition [10,11]. But its existence in the coating triggered inferior mechanical properties in HVOF deposited HA coatings [8], which was believed to be the most important factor determining its durability. For adequate long-term usage, HA coating must not only have either surface characteristics that allow bone to grow into the surface and become mechanically locked or have surface chemical properties that promote the chemical attachment of bone to it. Instead, the mechanical properties of materials used in the construction of the prosthesis must also be appropriate. Once the bioactivity of HA implants is ascertained the mechanical property is the most important variable, which ultimately determines its duration. To date, interfacial mechanical strength between bone and HA coating has been extensively investigated in vivo in terms of adhesive/shear strength [12–15]. HA coating degradation was generally disclosed. The degree of HA degradation determines the ultramorphological appearance and ultrastructure of the bone/HA bond [1]. Therefore, it is a prerequisite to reveal the in vitro response of HVOF sprayed HA coatings when considering future application, especially to clarify the degradation of coating mechanical properties on the basis there are so far no publications on in vitro study of HVOF sprayed HA coatings.

In the present study, the in vitro behavior of HVOF HA coatings was involved to clarify the ageing effect on coating structure and phase composition as well as flexural modulus. The HA coatings were incubated in SBF with comparative composition to human blood plasma and the changes of surface phase composition and dissolution/precipitation behavior were investigated. The degradation in flexural modulus of HA coatings attributed to immersion in the SBF was studied using a 3-point bending test.

2. Materials and experimental procedures

A previous paper [8], details how coating samples were prepared by HVOF onto Ti–6Al–4V substrates with spray-dried HA powder made by a wet chemical method as feedstock. The starting HA powder was heat-treated in furnace at 900°C air for 1.5 h and fully crystalline HA structure was ascertained before coating deposition. A fully computerized *HV2000* HVOF (Praxair, USA) system with a nozzle diameter of 19 mm was used for the coating preparation. Hydrogen was utilized as the fuel gas with a flow rate of 566 l/min. The flow rate of oxygen was 283 l/min. Powder carrier

Table 1
Composition of the SBF with the comparison to human blood plasma

Ion	Ion concentration (mM) (SBF)	Ion concentration (mM) (Blood plasma)
Na^+	142.0	142.0
K^+	5.0	5.0
Mg^{2+}	1.5	1.5
Ca^{2+}	2.5	2.5
Cl^-	147.8	103.0
HCO_3^-	4.2	27.0
HPO_4^{2-}	1.0	1.0
SO_4^{2-}	0.5	0.5

gas was argon with a flow rate of 19 l/min and the powder feed rate is 6 g/min. The spray distance was set at 250 mm. Two types of HA coatings, coating A (starting powder size: $30 \pm 5 \, \mu m$) and coating B (starting powder size: $50 \pm 5 \, \mu m$), were investigated. The phase compositions of these two coatings are shown in Figs. 4(a) and 5(a), respectively. The small coating samples used for in vitro test were of the dimension 12 mm × 12 mm in width and length, respectively. And the coating thickness was around 100 μm.

The ion concentrations of the SBF (pH = 7.40) is tabulated in Table 1 with comparison made to corresponding human blood plasma. The in vitro test was conducted in a continuously stirred bath containing distilled water with a stable temperature of 37°C. Each coating sample was incubated in 70 ml of SBF contained in a polyethylene bottle. For each test group, three samples were used. Once the sample was taken out from the solution, it was washed in distilled water and subsequently dried at ambient temperature. The coating samples were weighed before and after immersion in the solution.

Coating surface morphology was observed by scanning electron microscope (SEM, JEOL JSM-5600LV). X-ray diffraction (XRD) analysis (MPD 1880, Philips, Netherlands) was conducted to reveal the phase changes on the coating surface after different incubation duration. The operating conditions were 40 kV and 30 mA by using Cu Kα radiation. The goniometer was set at a scan rate of 0.015°2θ/s over a 2θ range of 20–60°. The concentration of Ca^{2+} in the SBF was measured by inductively coupled plasma (ICP, Perkin-Elmer, Emission Spectrometer Plasma 400, USA) spectroscopic analysis. Four sets of data were obtained for an average value for each type of SBF sample.

The 3-point bend test [16] was conducted on a universal testing machine for the determination of flexural modulus of HA coating after immersion in the SBF for 7, 14, 21, 28, 35 and 42 days. The coating sample was of the dimension of 180 μm × 20 mm × 100 mm in thickness, width and length, respectively. The
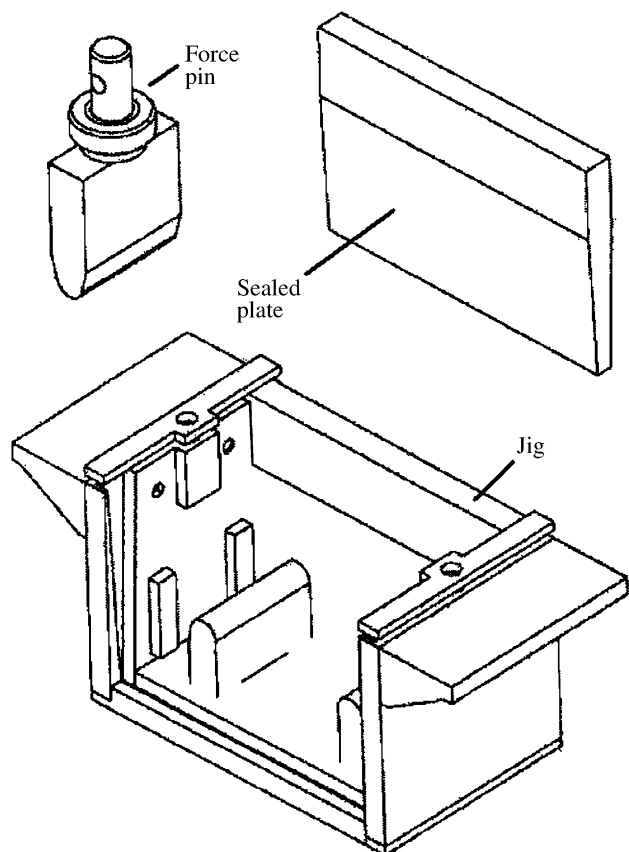
Fig. 1. Schematic three-dimensional depiction of the Jig for Young's modulus determination by using 3-point bending test.

substrate, Ti–6Al–4V plate was 2 mm thick. The loading rate was 0.2 mm/min and in the elastic deformation stage, a set of load-deflection data was chosen for the determination of flexural modulus. The SBF was renewed once a week. As a matter of fact, during the testing, coating samples should not be separated from the SBF, thus an experimental jig for 3-point bend test in vitro was designed and manufactured in AISI 316L stainless steel, which is schematically shown in Fig. 1 for the present study.

3. Results

The surface morphology changes with immersion duration in coating A and coating B are demonstrated in Figs. 2 and 3, respectively. Fig. 3(h) shows the fine surface microstructure of the precipitated layer. Significant difference exists between these two coatings in terms of surface morphology modifications to immersion duration. For coating A, it is found that after 6 h immersion in the SBF, notable changes occur on coating surface as shown in Fig. 2(b). Also from the SEM image (Fig. 2(b)), a trace of oriented dissolution on HA

coating surface is evident. Augmented phenomenon is demonstrated after 24 h immersion in SBF (shown in Fig. 2(c)). Precipitation is gradually demonstrated. The coating surface is completely covered by the precipitates 3 days later. However, for coating B, which is made from larger powder than coating A, 6 h of immersion brings about no obvious changes and apparent dissolution is only confirmed after 3 days as shown in Fig. 3(d). After 7 days of immersion, distinct phase precipitation on coating B surface is demonstrated. Moreover, in this period of time, the coating surface is still not fully covered by the precipitated layer. From the view of topographical morphology of coatings, it is found that the surface morphology changes of HA coatings are very dependent on immersion duration and the growth of attached materials show the growth mechanism of net-shape connection with honeycomb-like surface structure, as shown in Fig. 3(h).

XRD patterns of the coatings after immersion at different duration are depicted in Figs. 4 and 5. In coating A, the most obvious change occurs after an incubation of 7 days. It is found that the α-TCP and β-TCP in the coating gradually diminished and eventually disappear completely. Compared to coating A, except for the quick disappearance of tetracalcium phosphate (TTCP), coating B shows delayed phase changes. TCP dissolves completely after 14 days of incubation. In coating A, the amorphous phase is replaced by a crystalline structure after 3 days of in vitro ageing. The final phase formed upon the coating surface is bone-like hydroxyapatite with some amorphous phases, which has been revealed by many researchers with nearly the same structure as natural bone [17]. The XRD analysis results correspond well to the surface morphology shown in Figs. 2 and 3.

Fig. 6 shows the influence of immersion duration on weight changes in the coatings. Distinct changes are revealed for coatings A and B with incubation time of less than 24 h. Coating A shows weight decrease while coating B demonstrates a slight weight increase. After approximately 3 days of immersion, the coatings demonstrate weight-increasing characteristics and the rate is nearly the same. It is found that prior to the 14th day, the precipitation of bone-like apatite on the surface of coating A, which has more amorphous phase, proceeded faster than coating B.

The changes of Ca^{2+} concentration in the SBF after different immersion duration are shown in Fig. 7. At the beginning of the incubation, both coatings revealed increase in Ca^{2+} concentration. After the 3rd day, it starts to decrease. Coating A shows more significant change than coating B. It should be noted that coating A demonstrated a significant drop prior to the slow descend.

The effect of in vitro incubation on the flexural elastic modulus of HA coatings is shown in Fig. 8. It should be
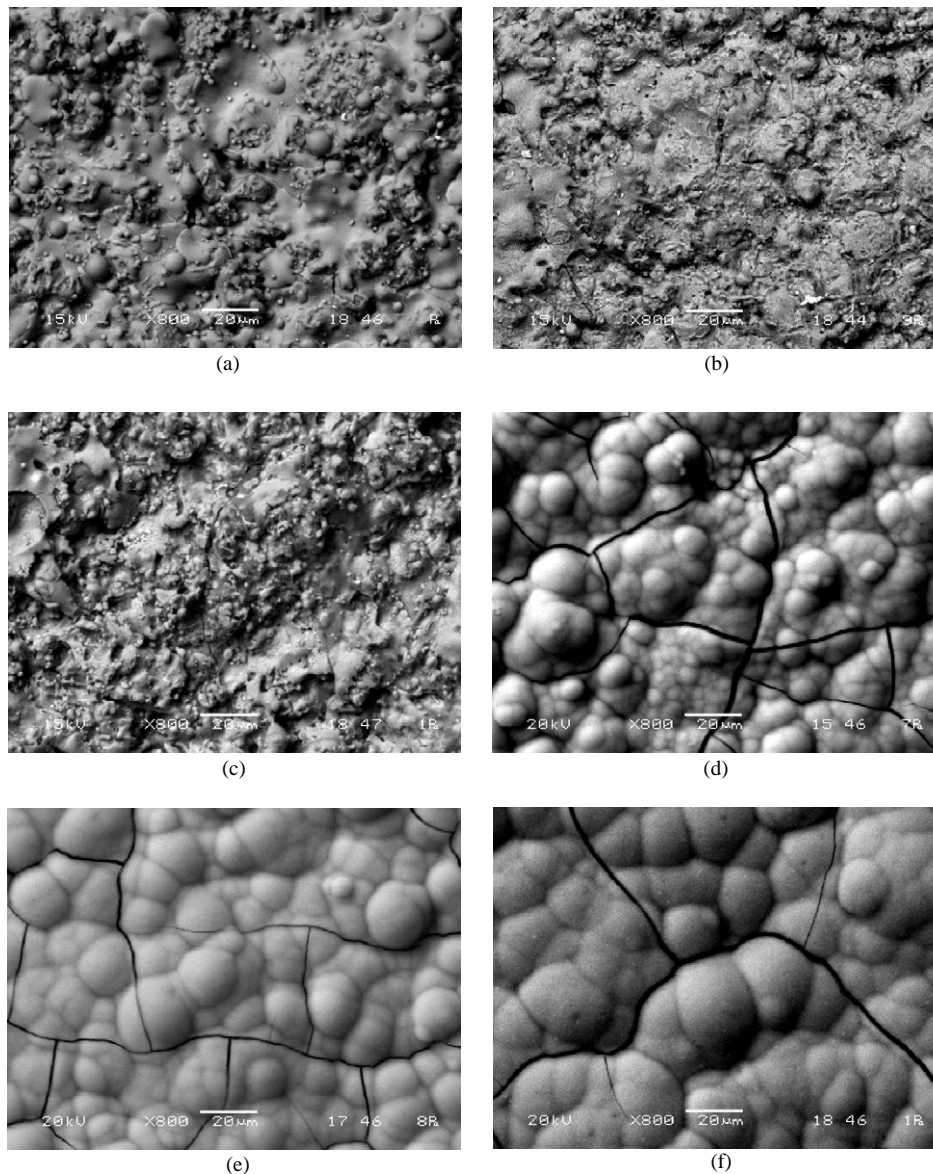
Fig. 2. Surface morphology changes of coating A ageing in the SBF with the immersion time of: (a) 0 h; (b) 6 h; (c) 1 day; (d) 3 days; (e) 7 days; and (f) 14 days, showing that after 3 days incubation coating surface has been fully covered by precipitated layer.

noted that prior to each flexural modulus determination from the load-deflection curve obtained from the 3-point bend test, the coating thickness was accurately re-measured by using micrometry. This is because the determination of flexural modulus is related to the actual coating thickness [16]. For coating A, the modulus shows an increase from 20.55 ($\pm$1.55) to 30.01 ($\pm$2.10) GPa after 7 days and decreases progressively as the immersion duration. However, for coating B, following similar decreases in flexural modulus after the 7th day, no further alternation can be seen as the immersion time prolongs. After 21 days ageing, both the coatings show approximately the same trend.

4. Discussion

HA coatings with a reasonable content of amorphous phase show that the dissolution–reprecipitation equilibrium with the solution appeared to be reached within 48 h [3]. Present results correspond well to those findings. Figs. 2 and 3 reveal that coatings A and B demonstrate different dissolution/precipitation rates. Predominantly due to different phase compositions that resulted from having different melt fraction of HA [8]. It reveals that phase composition significantly determines the dissolution and precipitation behavior. The gradual disappearance of TCP and amorphous calcium
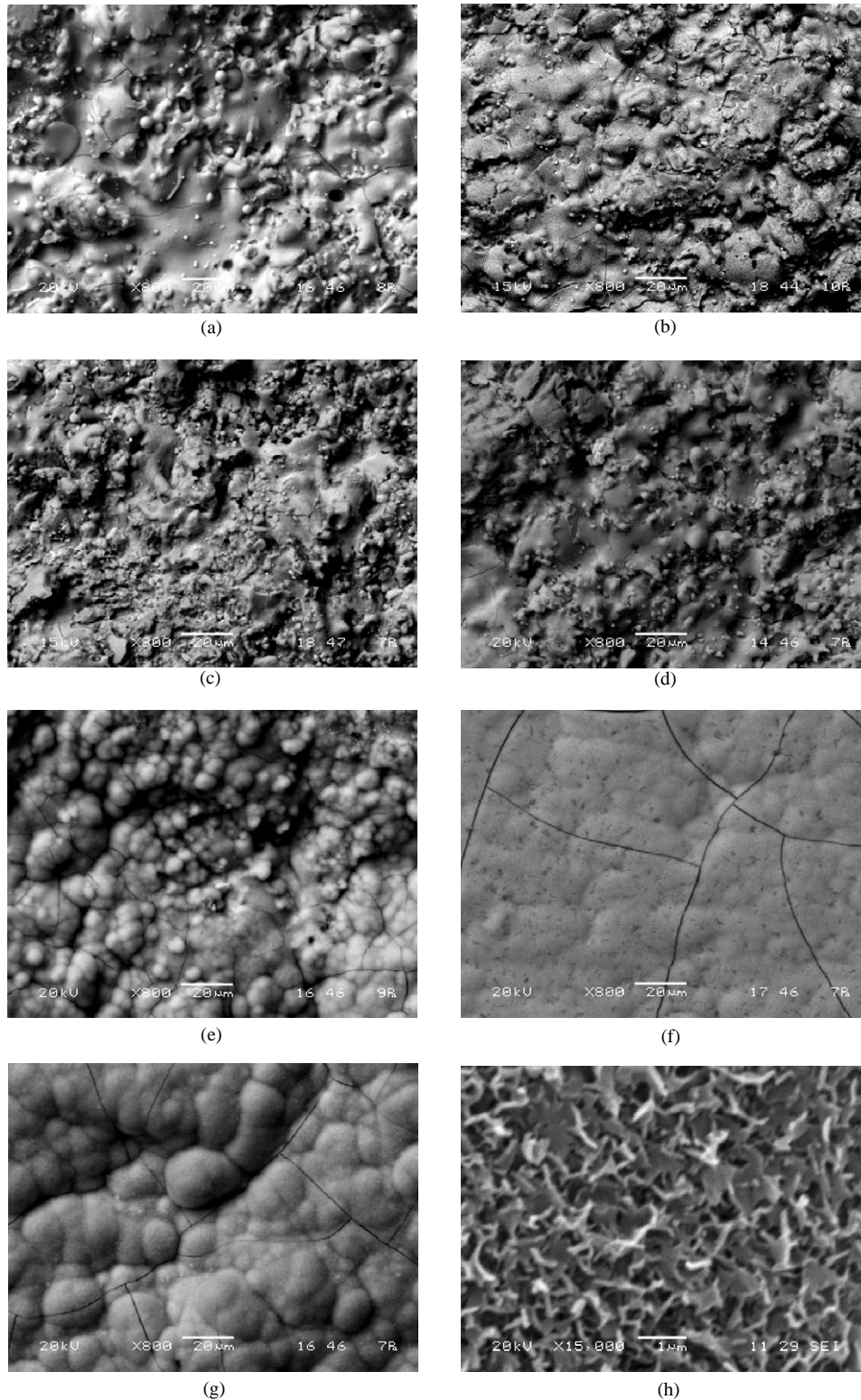
Fig. 3. Surface morphology changes of coating B ageing in the SBF with the immersion time of: (a) 0 h; (b) 6 h; (c) 24 h; (d) 3 days; (e) 7 days; (f) 14 days; (g) 21 days; and (h) shows the structure of attached layer.

phosphate (ACP) shows the dissolvability of the phases in HA coating, that is, TCP and ACP have higher dissolvability than HA, as claimed by previous work [4,5]. And the quick disappearance of TTCP shown in Fig. 5 confirms the reported findings that TTCP has the highest dissolvability among the calcium phosphate
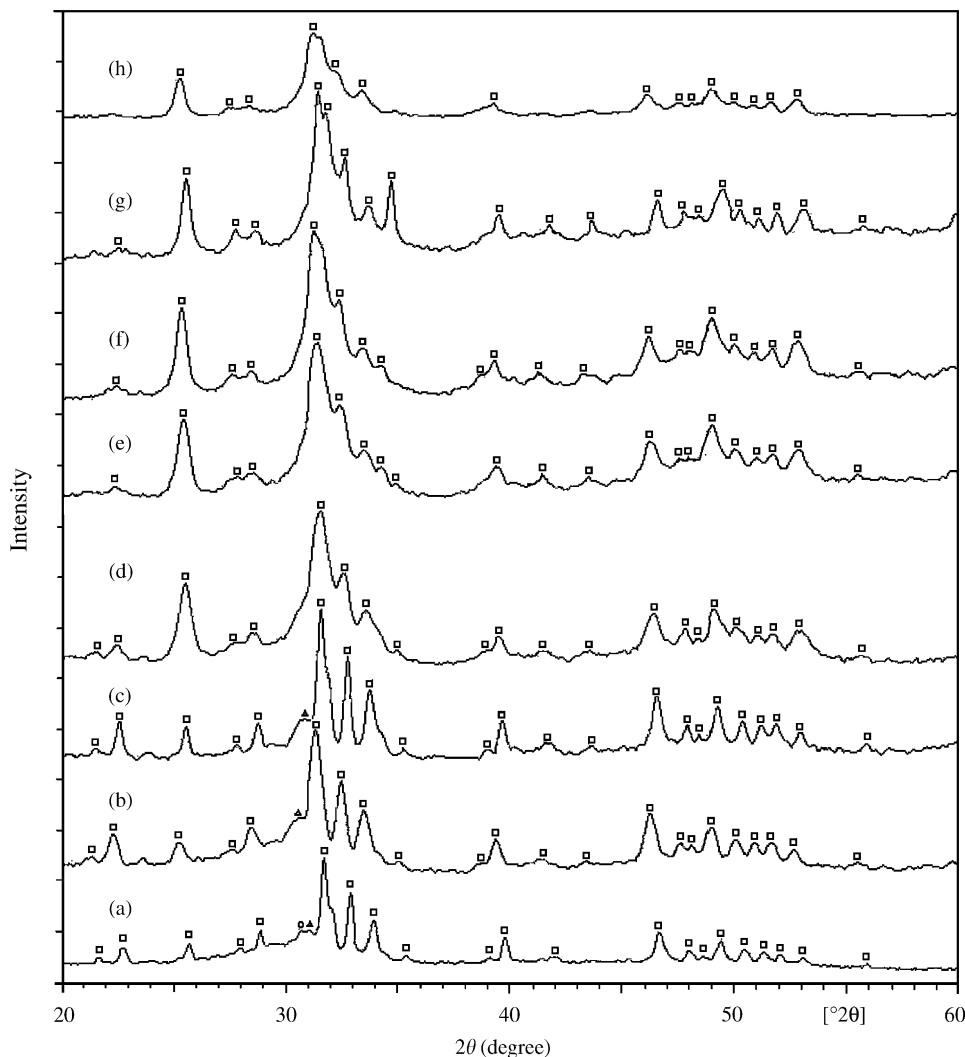
Fig. 4. XRD patterns of coating A showing the changes of surface phase composition with the immersion periods of time in the SBF (□—HA). ○—α-TCP and △—β-TCP gradually diminished till disappeared, with the immersion time of (a) 0 h, (b) 6 h, (c) 24 h, (d) 3 days, (e) 7 days, (f) 14 days, (g) 21 days and (h) 28 days.

compounds. The dissolution rate is, in ascending order, as follows [4]:

$$\beta\text{-TCP} < \alpha\text{-TCP} < \text{amorphous calcium phosphate} < \text{TTCP}.$$
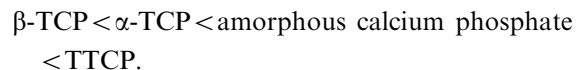
It should be noted that CaO is likely formed in the coatings, as a result of HA's thermal decomposition during coating deposition. Its existence could contribute to the overall dissolution behavior of the coatings at the initial stage. However, due to its apparent limited quantity in the coatings, it could not be evidently detected by the present XRD technique where the detection limit is ~1 wt%. Dissolution behavior of HVOF sprayed coatings in the present study reflects their phase composition. In coating A, the rapid dissolution indicated by the surface morphology in Fig. 2(a, b) is responsible for the decrease in coating weight after 6 h of immersion and further decrease after

24 h of ageing. In coating B, the continuous weight increase indicates that the dissolution of the calcium phosphate coating is limited. And once the dissolution/ precipitation equilibrium is achieved, the dissolution is decidedly minimized. Actually, the coatings with a high dissolution rate support the growth of bony tissue owing to the dissolved calcium and phosphorus ions [18]. Several studies have defined the importance of an early dissolution of HA coatings during apposition of bony tissues onto the implants [2,19].

The favorable effect on bone apposition on the HA implant gives evidence that this is due to early adhesion of osteoblasts and direct deposition of bone matrix on the HA substrate [2]. Thus, advanced precipitation on the HA coating surface can be beneficial. According to this viewpoint, the existence of certain content of amorphous phase is thus favorable. However, the incubation duration when dissolution/precipitation
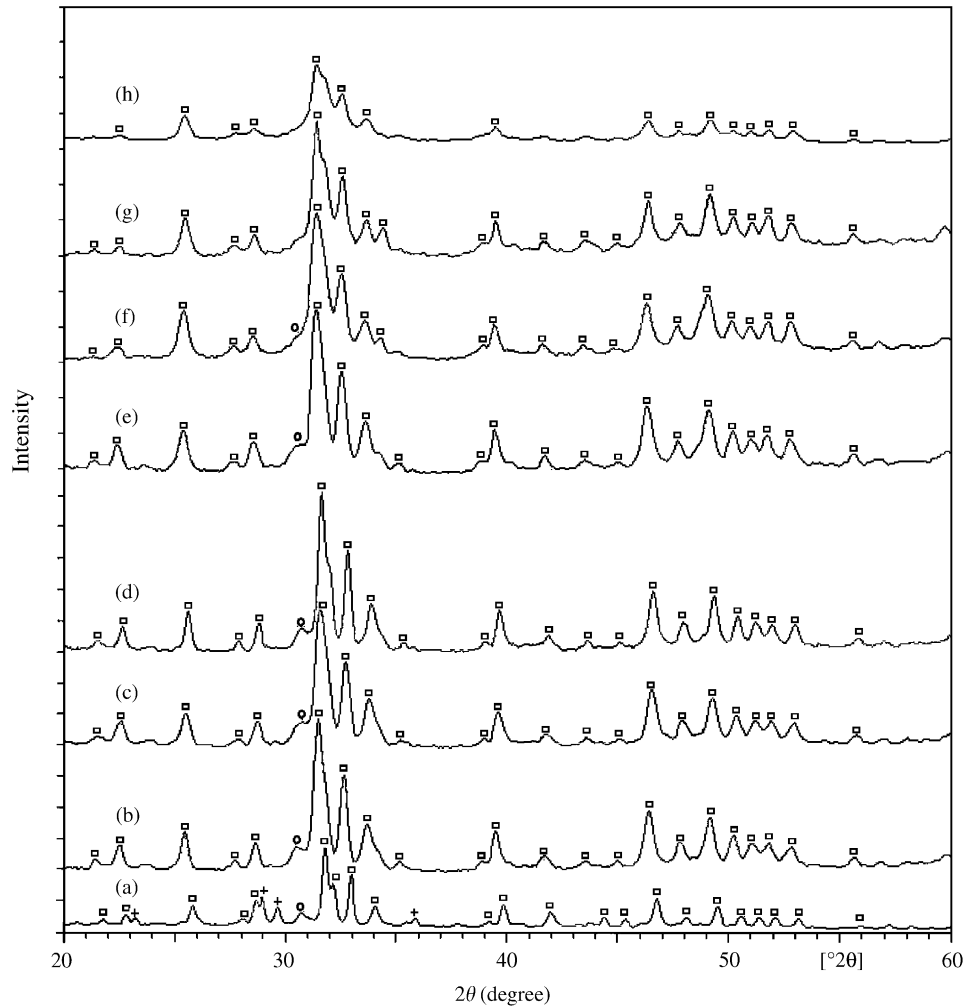
Fig. 5. XRD patterns of coating B showing the changes of surface phase composition with the immersion periods of time in the SBF (□—HA). ○—α-TCP and +—TTCP gradually diminished till disappeared, with the immersion time of (a) 0 h, (b) 6 h, (c) 24 h, (d) 3 days, (e) 7 days, (f) 14 days, (g) 21 days and (h) 28 days.

reaches equilibrium appears to be important. And concerning comparative dissolution rates of TCP indicated by the XRD patterns, shown in Figs. 4 and 5; it seems that the existence of ACP has some influence in accelerating the dissolution of TCP. It was reported that most of the resorbed Ca^{2+} had reprecipitated onto the coating as an amorphous phase [20]. The present study confirms this. At the beginning of the incubation of HA coatings in the SBF, the increase of Ca^{2+} concentration comes predominantly from the release of Ca^{2+} from the HA coating. The quick dissolution for the coatings suggests that the initial high rate of ion uptake rate decrease after 24 h.

For coating A, the sharp decrease after 3 days of ageing shown in Fig. 8 indicates the rapid precipitation of the bone-like apatite from the SBF, which was confirmed by the corresponding significant weight increase as seen in Fig. 6. After 7 days, both coatings exhibit decreasing trend in Ca^{2+} concentration indicat-

ing that precipitation has gradually taken place. However, even after prolonged incubation periods in the SBF, the HA coatings do not demonstrate a near-linear weight increase pattern. This may be attributed to the continuous dissolution accompanying precipitation during the entire in vitro test. And the gradual decrease in Ca^{2+} concentration in the SBF is also responsible for the laggard alterations. The cracks shown in Fig. 9 could more or less contribute to the further dissolution of Ca^{2+} in that the ions could be released through the cross-thickness cracks. It should be noted that, compared to as-sprayed coating, the coating surface exhibits identified connected cracks after some immersion time ageing in the SBF, which can be observed from Fig. 2(c)–(f) and Fig. 3(d)–(g). The comparison of the coating surface morphology during the early stages of immersion (Figs. 2(b) and 3(b), (c)) reveals that the cracks existing on the coating surface come mostly from the original crack in as-sprayed coating. It is also found
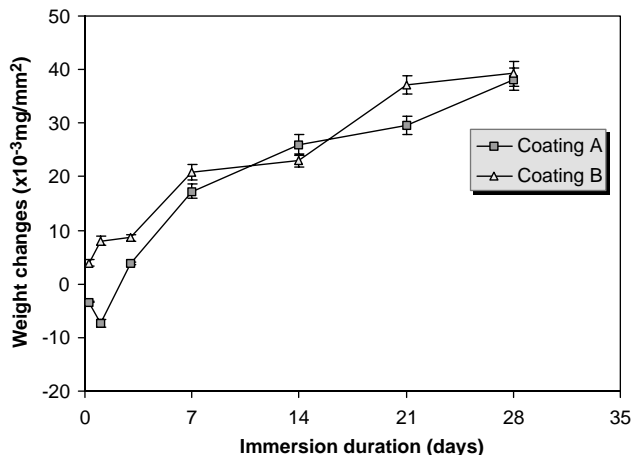
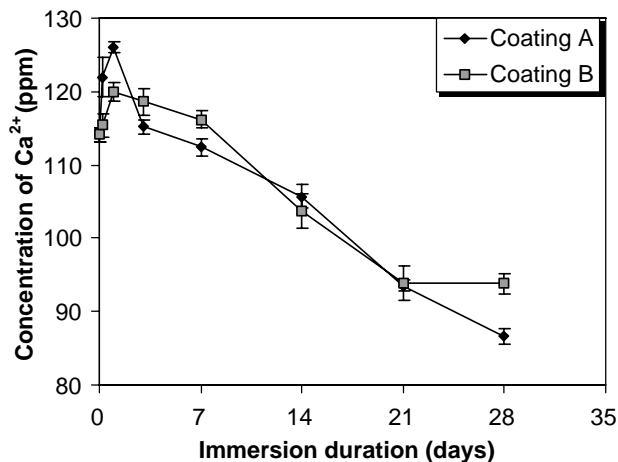Fig. 6. Weight changes of HA coating samples via immersion duration in the SBF.

Fig. 9. Typical crack morphology located on HA coating surface after the ageing time of 21 days.

Fig. 7. Ca^{2+} concentration in the SBF via immersion duration of coating samples.
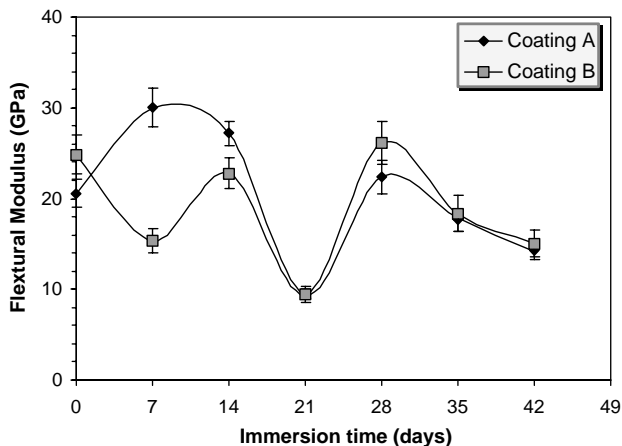
Fig. 8. Influence of in vitro ageing on the flexural modulus of HVOF sprayed HA coatings.
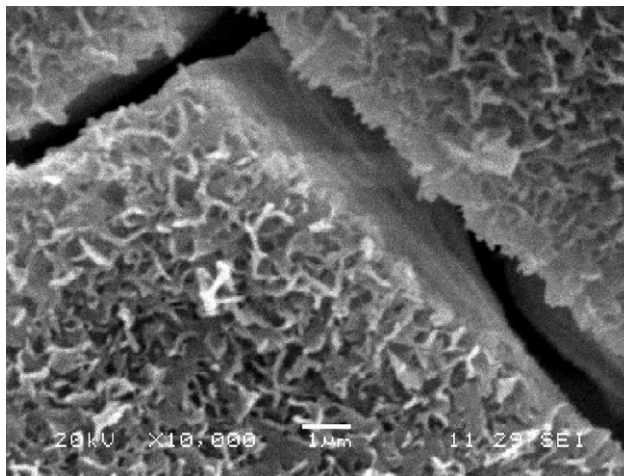
that the crack density decreases with elongation of immersion duration. Even though the precipitated layer can fill some microcracks, the relatively large cracks prevailed. It is possible that dissolution of the phases located around the crack edges also contributes to the widened crack.

Extensive studies revealed that the coating's dissolution rate was dependent on crystallinity, composition, structure, surface area, and density [6]. It should be pointed out that the dissolution and precipitation have oriented characteristics, which is revealed in Fig. 10. It was believed that the dissolution of the α-TCP could favor the precipitation of the poorly crystallized apatite phase in the coating while for the HA coating the absence of dissolution would delay this precipitation [21]. The precipitation always takes place at the locations where dissolution occurred. It was believed that accumulation of precipitated hydroxyapatite involves the first attachment of molecule on coating surface. The oriented dissolution and precipitation are likely to be triggered by concrete phase composition of HA coating, and this can be elucidated by analysis of single splats. Fig. 11 shows the in vitro behavior HA splats with 3 days incubation. The splat was deposited on a polished Ti–6Al–4V plate by using the same HVOF spray process as coating A and coating B. A shield plate was placed between the substrate and HVOF flame to collect single HA splats and several holes of 1 mm in diameter were drilled on the shield plate for this purpose. Sieving procedure was carried out for the preparation of different starting HA powder in terms of small particle size range.

The well-flattened splat morphology suggests that HA particles attained fully melted state during the HVOF spray. It is found that the original particle size determines its dissolution rate realized through its melt state. For small HA particles that fully melt in the
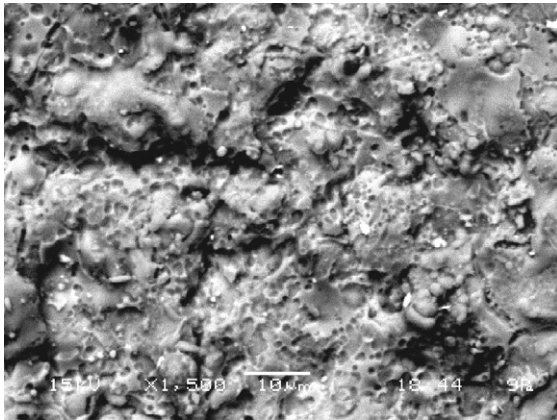
(a)
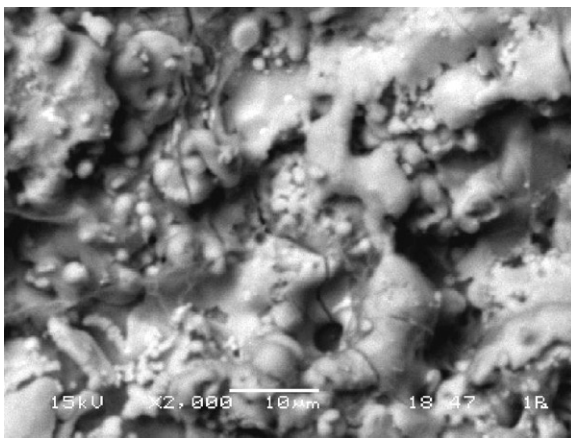
(b)

Fig. 10. SEM image of coating A surface in high magnification showing: (a) the oriented dissolution with 6 h ageing; and (b) the oriented precipitation with the ageing time of 24 h in the SBF.

HVOF flame, the resultant splat virtually disappeared indicating complete dissolution before any precipitation can commence, as shown in Fig. 11(a-2). With the augmentation of particle diameter, the images clearly demonstrate that the surrounding parts of the splats disappear while the core remained and some precipitation can be validated. As the particle diameter reached $\sim 70\,\mu m$ as shown in Fig. 11(e), no obvious dissolution is discernible. It has been discussed that TCP and amorphous phase in the as sprayed HA coatings came mainly from melted particle [8]. During in vitro ageing, TCP and amorphous calcium phosphate dissolve preferentially in the SBF. It is believed that the unmelted part contains mostly crystalline structure that remained from the starting particle during coating formation. Considering the phase-oriented dissolution in SBF (Fig. 10), the outer layer of single HA splats should contain more dissolvable phases, such as TCP, amorphous calcium phosphate, etc., than the sub-terrain layer. The phases coming from HA phase transformation exist mostly around the core based on the

consideration that at elevated temperatures, phase transformation occurs [22,23]. The resultant phases should be responsible for the dissolution during immersion in SBF. The whole procedure of single HA splat behavior in the SBF is schematically portrayed in Fig. 12. And the oriented dissolution/precipitation is the reason why the attached layer is found to have altered thickness, and confirms that further dissolution is one reason triggering the enlargement of cross-thickness cracks. In this viewpoint, fully melted state of HA particles is not suitable and partially melted state is preferred. It is thus obvious that, compared to conventional plasma spray process, which result in significant HA phase decomposition and hence higher relative content of TCP, ACP, etc., in the resultant coatings, the present HVOF is competitive in depositing the calcium phosphate coatings with the capability of quick precipitation.

As mentioned, it is an interesting phenomenon that precipitation originally occurs at the region where dissolution took place. As a matter of fact, bulk bone-like apatite layer formation should originally come from first attachment of single molecule. For simplicity, a molecule, P, is considered to be spherical as it approaches a solid surface in liquid. Suppose that it stick or adhere to the surface. The work of adhesion is then expressed as (for adhesion of phase A to B) [24]

$$W_{AB} = \gamma_A + \gamma_B - \gamma_{AB}, \tag{1}$$

where γ_A and γ_B are free surface tensions, γ_{AB} is interfacial surface tension. For this situation, it can be written as

$$W_{SP} = \gamma_{SL} + \gamma_P - \gamma_{PS}. \tag{2}$$

The value of W_{SP} must be negative for adhesion to take place (S represents solid, L represents liquid, and P is the molecule). Kinetic rate law has been used for the explanation of dissolution behavior in the SBF [4]. The precipitation mechanism involves the determination of free surface tensions of TCP and HA, as well as the bone-like apatite. It has been reported that apatite is the most thermodynamically favored phase to precipitate (it has the highest negative Gibbs free energy value) [21]. Further investigation is needed. It is obvious that the surface dissolution is one of the steps leading to calcium phosphate precipitation and subsequent tissue bonding. The precipitation rate depends extensively on how much fresh surface is supplied. And once the coating surface is completely covered by the attached spheres, further dissolution is decidedly minimized.

Besides the consideration of W_{SP}, the concentration difference of Ca^{2+} should be simultaneously considered. The large concentration difference brought mainly by dissolution is the reason why at early incubation stage precipitation rate is high, as indicated by Figs. 6 and 7.
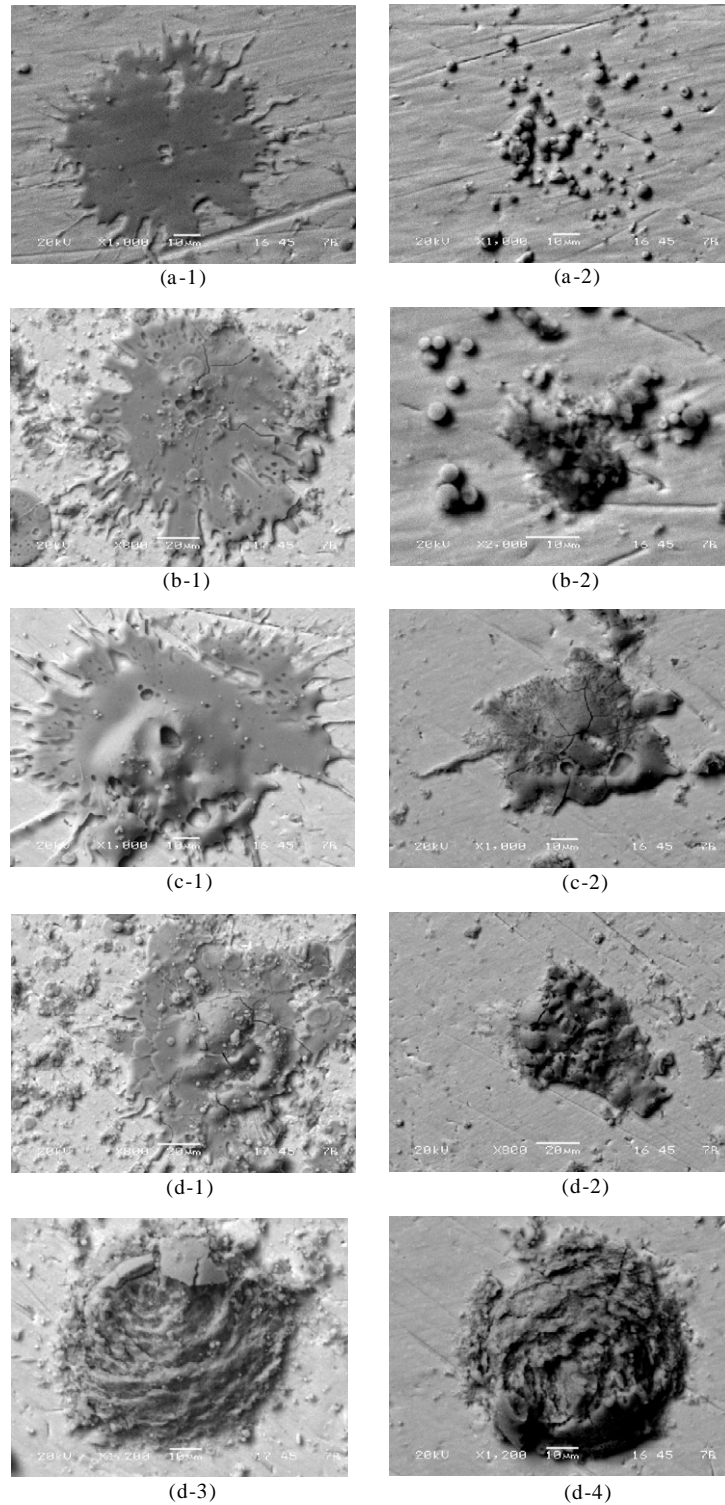
Fig. 11. SEM images of HA splats before (−1) and after (−2) immersed in the SBF with 3 days showing the effect of particle size on the dissolution/ precipitation behavior, the particle size is increased from around 25 μm to nearly 70 μm corresponding to image (a)–(e).

It is believed that the calcium phosphate ceramics undergo dissolution, re-precipitation, and/or ion exchange reactions leading to a bone-like apatite surface as one of the steps leading to enhanced bone tissue formation and bone bonding. And the degree of HA degradation determines the ultramorphological appearance and ultrastructure of the bone/HA bond [25] thus determines the bonding strength of the implants to bone. So the dissolution rate must be considered once the coating is implanted into the body. It was pointed
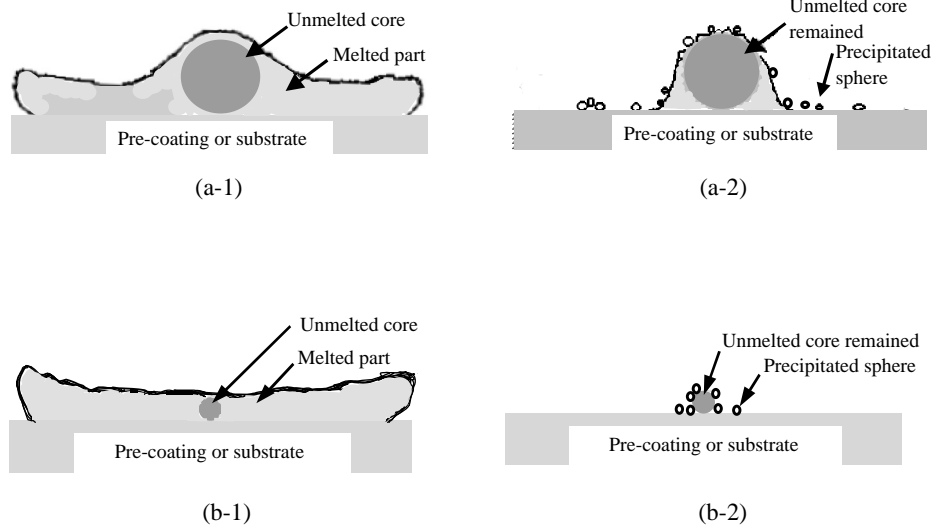
Fig. 12. Schematic illustration of HA splats behavior in vitro with 3 days ageing showing that surrounding melted part nearly totally dissolved and only the unmelted core is remained: (−1) is the original splat; and (−2) is the corresponding aged morphology. The decrease of HA particle size, (b) compared to (a), causes further phase dissolution.

out that the amount of Ca dissolved from Ca/P-coated implants was strongly dependent on the chemistry of the coating and less dependent on pH or time of incubation [20]. However, concerning the inhomogeneous layered structure of HA coatings, the incubation duration should play a role on the amount of dissolved Ca through the transverse cracks.

It is believed that the release of internal residual stresses within the coatings is responsible for the change in interlamellar and/or intralamellar cracks. The changes of residual stress can be confirmed by the shift of XRD peaks shown in Figs. 4 and 5, which could be used for the determination of residual stress in thermal sprayed coatings [26]. The dissolution at the coating surface is capable of releasing the constraint and thus is responsible for the changes in residual stresses. Generally, after HA coating deposition, residual tensile stress exists within HA coating and it can alter the concentration of supernatant species in solution, tensile stresses enhancing dissolution and compressive stresses impeding dissolution of the coating [27]. This phenomenon can be the partial reason why the dissolution is fast at the initial stage of immersion.

It is well known that Young's modulus (E) of materials depends on the bonding strength among atoms. Coating structure significantly influences the Young's modulus of thermally sprayed coating [28,29]. In addition, the residual stress existing in materials also plays an important role in determining the E value [30]. In the present study, the 3-point bend test simulates a macro-testing method and thus the E values obtained reflects the whole characteristic of the HA coatings. The E values demonstrate a complicated trend, which may be attributed to the overall influence of coating
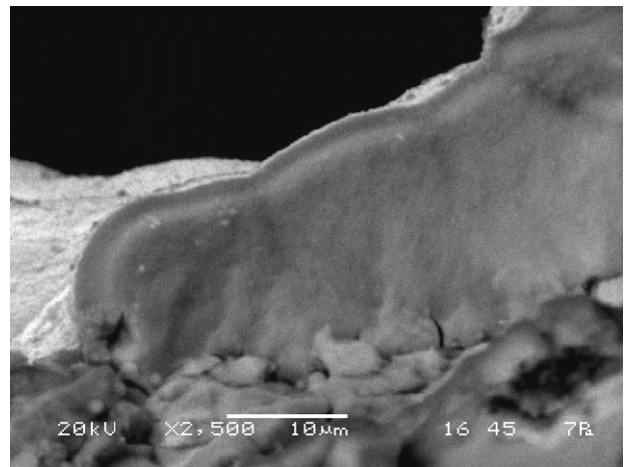

Fig. 13. Typical cross-sectional morphology of precipitated hydroxyapatite showing very dense structure. The SEM images were obtained from coating A after immersion time of 21 days.

structure, including phase composition, and residual stress. The initial dissolution at the coating's surface, which results in the releasing of residual stress, is likely to be responsible for the decrease in E values of coating B. It has been found that E values of HA is lower than that of TCP [30] and HA should have different E values from amorphous calcium phosphate. The dissolution of TCP and amorphous phase also contribute to the decreased E. From the cross-sectional investigation of the precipitated layer shown in Fig. 13, it is obvious that the attached layer has a dense structure and bonds with HA coating firmly. The dense structure is the reason for the enhancement of E value in coating A after 7 days incubation considering that the pores existing in the

coating are detrimental for the E [28]. The low E values demonstrated after 21 days immersion may be resulted from further release of residual stresses. Once the precipitated layer fully covers the coating surface, the changes of E value diminish, as shown in Fig. 8 at 35 and 42 days, and, as could be predicted, remained stable. It is known that the E value of cortical bone is around 7–30 GPa [31], the present HVOF HA coatings show comparative values.

5. Conclusions

The dissolution/precipitation rate of HVOF sprayed HA coatings is found to be significantly dependent upon coating phase composition, which can be altered through adjusting the starting HA powder size. It is revealed that dissolution is a necessary step leading to the precipitation of bone-like hydroxyapatite on the HA coatings. During in vitro ageing, the release of residual stress and subsequent changes in the microstructure and surface phases result in the changes of HA coatings in terms of Young's modulus and no obvious degradation can be observed. Incubation of HA splats in the SBF shows that the dissolution occurs mostly around the outermost perimeter of the splats where the majority of the amorphous phases reside. And before the occurrence of initial precipitation, the dissolution cannot be minimized. To achieve rapid precipitation, partial molten state of HA particle during coating deposition was suggested.

Acknowledgements

References

[1] Bagambisa FB, Joos U, Schilli W. Mechanisms and structure of the bond between bone and hydroxyapatite ceramics. J Biomed Mater Res 1993;27:1047–55.

[2] Pazzaglia UE, Brossa F, Zatti G, Chiesa R, Andrini L. The relevance of hydroxyapatite and spongious titanium coatings in fixation of cementless stems, An experimental comparative study in rat femur employing histological and microangiographic techniques. Arch Orthop Trauma Surg 1998;117:279–85.

[3] Radin SR, Ducheyne P. The effect of calcium phosphate ceramic composition and structure on in vitro behavior, II. Precipitation. J Biomed Mater Res 1993;27:35–45.

[4] Ducheyne P, Radin S, King L. The effect of calcium phosphate ceramic composition and structure on in vitro behavior, I. Dissolution. J Biomed Mater Res 1993;27:25–34.

[5] Harada Y, Wang JT, Doppalapudi VA, Willis AA, Jasty M, Harris WH, Nagase M, Goldring SR. Differential effects of different forms of hydroxyapatite and hydroxyapatite/tricalcium phosphate particulates on human monocyte/macrophages in vitro. J Biomed Mater Res 1996;31:19–26.

[6] Wise DL, Trantolo DJ, Kai-Uwe L, Gresser JD, Cattaneo MV, Yaszemski MJ. Biomaterials engineering and devices: human applications, Vol. 2: orthopedic, dental, and bone graft applications. Totowa, NJ: Humana Press, 2000.

[7] Munting E. The contributions and limitations of hydroxyapatite coatings to implant fixation: a histomorphometric study of load bearing implants in dogs. Int Orthop (SICOT) 1996;20:1–6.

[8] Li H, Khor KA, Cheang P. Effect of powders' melting state on properties of HVOF sprayed hydroxyapatite coatings. Mater Sci Eng A 2000;293:71–80.

[9] Haman JD, Chittur KK, Crawmer DE, Lucas LC. Analytical and mechanical testing of high velocity oxy-fuel thermal sprayed and plasma sprayed calcium phosphate coatings. J Biomed Mater Res 1999;48:856–60.

[10] Maxian SH, Zawadsky JP, Dunn MG. Mechanical and histological evaluation of amorphous calcium phosphate and poorly crystallized hydroxyapatite coatings on titanium implants. J Biomed Mater Res 1993;24:717–28.

[11] Frayssinet P, Tourenne F, Rouquet N, Conte P, Delga C, Bonel G. Comparative biological properties of HA plasma-sprayed coatings having different crystallinities. J Mater Sci Mater Med 1994;5:11–7.

[12] Oonishi H, Yamamoto M, Ishimau H, Tsuji E, Kushitani S, Aono M, Ukon Y. The effect of hydroxyapatite coating on bone growth into porous titanium alloy implants. J Bone J Surg 1989;10:213–6.

[13] Cook SD, Thomas KA, Dalton JE, Volkman TK, Whitecloud TS, Kay JF. Hydroxylapatite coating of porous implants improves bone ingrowth and interface attachment strength. J Biomed Mater Res 1992;26:989–1001.

[14] Thomas KA, Kay JF, Cook SD, Jarcho M. The effect of surface macrotexture and hydroxylapatite coating on the mechanical strengths and histologic profiles of titanium implant materials. J Biomed Mater Res 1987;21:1395–414.

[15] Wang S, Lacefield WR, Lemons JE. Interfacial shear strength and histology of plasma sprayed and sintered hydroxyapatite implants in vivo. Biomaterials 1996;17:1965–70.

[16] Li H, Khor KA, Cheang P. Titanium dioxide reinforced hydroxyapatite coatings deposited by high velocity oxy-fuel (HVOF) spray. Biomaterials 2002;23(1):85–91.

[17] Weng J, Liu Q, Wolke JQC, Zhang X, de Groot K. Formation and characteristics of the apatite layer on plasma-sprayed hydroxyapatite coatings in simulated body fluid. Biomaterials 1997;18:1027–35.

[18] Lugscheider E, Knepper M, Heimberg B, Dekker A, Kirkpatrick CJ. Cytotoxicity investigations of plasma sprayed calcium phosphate coatings. J Mater Sci Mater Med 1994;5:371–5.

[19] Hardy DCR, Frayssinet P, Delince PE. Osteointegration of hydroxyapatite-coated stems of femoral prostheses. Eur J Orthop Surg Traumatol 1999;9:75–81.

[20] Maxian SH, Zawadsky JP, Dunn MG. In vitro evaluation of amorphous calcium phosphate and poorly crystallized hydroxyapatite coatings on titanium implants. J Biomed Mater Res 1993;27:111–7.

[21] Cleries L, Fernandez-Pradas JM, Morenza JL. Behavior in simulated body fluid of calcium phosphate coatings obtained by laser ablation. Biomaterials 2000;21:1861–5.

[22] Gross KA, Berndt CC. Thermal processing of hydroxyapatite for coating production. J Biomed Mater Res 1998;39:580–7.

[23] Zhou J, Zhang X, Chen J, Zeng S, de Groot K. High temperature characteristics of synthetic hydroxyapatite. J Mater Sci Mater Med 1993;4:83–5.

[24] Black J. Biological performance of materials, fundamentals of biocompatibility, 3rd ed. Revised and expanded. New York: Marcel Dekker, Inc., 1999.

[25] Reis RL, Monteriro FJ. Crystallinity and structural changes in HA plasma-sprayed induced by cyclic loading in physiological media. J Mater Sci Mater Med 1996;7:407–11.

[26] Clyne TW, Gill SC. Residual stresses in thermal spray coatings and their effect on interfacial adhesion: a review of recent work. J Therm Spray Technol 1996;5:401–18.

[27] Sergo V, Sbaizero O, Clarke DR. Mechanical and chemical consequences of the residual stresses in plasma sprayed hydroxyapatite coatings. Biomaterials 1997;18: 477–82.

[28] Sevostianov I, Kachanov M. Modeling of the anisotropic elastic properties of plasma-sprayed coatings in relation to their microstructure. Acta Mater 2000;48:1361–70.

[29] Leigh SH, Lin CK, Berndt CC. Elastic response of thermal spray deposits under indentation tests. J Am Ceram Soc 1997;80:2093–9.

[30] Metsger DS, Rieger MR, Foreman DW. Mechanical properties of sintered hydroxyapatite and tricalcium phosphate ceramic. J Mater Sci Mater Med 1999;10:9–17.

[31] Cowin SC, editor. Mechanical properties of bone: presented at the Joint ASME–ASCE Applied Mechanics, Fluids Engineering, and Bioengineering Conference, Boulder, CO, June. New York: American Society of Mechanical Engineers, 1981.